Human IL-Rβ chains form IL-2 binding homodimers

Anne-Hélène Pillet*, Olivier Juffroy*, Virginie Mazard-Pasquier*, Jean-Louis Moreau, Franck Gesbert, Patricia Chastagner, Jean-Hervé Colle, Jacques Thèze, Thierry Rose

Unité d'Immunogénétique Cellulaire, Département Infection et Epidémiologie, Institut Pasteur, Paris, France

Correspondence : T. Rose, Ph.D., Unité d'Immunogénétique Cellulaire, Département Infection et Epidémiologie, Institut Pasteur, 25 rue du Dr Roux, 75724, Paris Cedex 15, France
<rose@pasteur.fr>

Accepted for publication February 5, 2008

ABSTRACT. Two types of functional interleukin-2 receptor (IL-2Rα/IL-2Rβ/γc and IL-2Rβ/γc) have already been characterized in humans. Here we describe a new form consisting of IL-2Rβ/β homodimers that assemble spontaneously in the absence of γc. Co-transfection of COS-7 cells with constructs expressing IL-2Rβ chains tagged with either HA or MYC sequences results in the formation of IL-2Rβ:HA/IL-2Rβ:MYC complexes detectable by coimmunoprecipitation. The formation of these IL-2Rβ:HA/IL-2Rβ:MYC dimers is also observed in the absence of IL-2. Moreover, in COS cells expressing chimeras of IL-2Rβ fused to fluorescence reporters such as IL-2Rβ:ECFP and IL-2Rβ:EYFP, we also observed specific FRET at the surface of living cells, as expected for dimer formation. Transiently transfected COS-7 cells expressing IL-2Rβ bind ^{125}I-labeled IL-2 (homodimers, *Kd* = 1nM) as cells expressing both IL-2Rβ and γc chains (heterodimers, *Kd* = 1 nM). IL-2Rβ/IL-2Rβ could represent either a decoy receptor or a new form of IL-2R involved in signaling when γc expression is low.

Keywords: interleukin-2, IL-2R, receptor assembly, FRET

Interleukin-2 (IL-2) is a major cytokine that possesses inflammatory and immune properties [1-4]. It exerts its effects on many cell types including T and B lymphocytes, monocytes and NK cells. Its role in lymphocyte proliferation, activation-induced cell death and controlling homeostasis has been extensively studied [5-8].

The effects of IL-2 on its target cells are mediated by specific cell surface receptors made up of three chains (IL-2Rα, IL-2Rβ and γc). IL-2Rα (CD25, 55 kDa) binds IL-2 with a dissociation constant of about 10 nM [9, 10]; this chain possesses a very short cytoplasmic domain with only 13 residues. IL-2Rβ (CD122, 67-75 kDa) is shared by both IL-2 and IL-15 receptors; it has a large intracytoplasmic domain (286 residues) and plays a critical role in signal transduction [11-13]. The last component, γc (CD132, 55-60 kDa), is shared by IL-2, IL-4, IL-7, IL-9, IL-15 and IL-21 receptors [14], and recent evidence indicates that it is also implicated in the growth hormone receptor [15]. Its cytoplasmic domain consists of 86 residues. IL-2Rβ and γc are members of the same cytokine class I receptor family which is characterized by two immunoglobulin folds in their ectodomains, whereas IL-2Rα, with its homolog IL-15Rα, belongs to an unrelated family characterized by the presence of SUSHI domains [16]. Two functional IL-2R have so far been described in humans. When IL-2Rβ and γc associate, they form an intermediate affinity receptor common to IL-2 and IL-15, with a *Kd* of about 1 nM for IL-2. The expression of all three chains, *i.e.* IL-2Rα, IL-2Rβ and γc, leads to the formation of a high affinity receptor specific for IL-2 (*Kd* = 10 pM) [1-4].

After binding IL-2, the IL-2Rβ-γc heterodimers trigger early downstream signals that involve tyrosine phosphorylation of a large array of cell proteins by several protein tyrosine kinases (PTKs): p56lck, Syk and Janus kinases (Jak) [17-19]. Jak1 and Jak3 are constitutively associated with IL-2Rβ and γc, respectively. They induce the phosphorylation of IL-2Rβ Tyr510 to form a docking site for STAT5 (signal transducer and activator of transcription). After phosphorylation, STAT5 molecules dimerize and are translocated into the nucleus where they induce IL-2-dependent genes such as IL-2Rα [20, 21].

The structure of the IL-2/IL-2R complex was determined recently from extracellular fragments of IL-2Rα, IL-2Rβ and γc [22, 23]. It shows similar architecture and organization to that of the human growth hormone/receptor and erythropoietin/receptor complexes, with the addition of a third receptor component, the IL-2Rα chain, capping IL-2, out of reach of the IL-2Rβ and γc chains. No structural data are available for IL-2Rβ and γc cytoplasmic domains or for any homologous protein domains. Energy parameters have been documented for the assembly – in solution – of soluble fragments of IL-2Rα, IL-2Rβ and γc ectodomains in the presence and absence of IL-2 [24].

The current view concerning the structure and function of the IL-2R as a heterotrimeric complex supposes the

* Contributed equally to this work.

doi: 10.1684/ecn.2008.0120

equimolar expression of each of the three IL-2Rα, IL-2Rβ and γc chains, though this is obviously not always the case [22, 24]. Therefore, we considered it important to study possible interactions between IL-2Rβ chains under conditions where IL-2Rβ is highly expressed and γc poorly expressed. We have previously demonstrated that the IL-2 mimetic P1-30 peptide is able to bind to the extracellular domain of IL-2Rβ assembled as a homodimer, as shown by analytical ultracentrifugation in solution, with a dissociation constant of the homodimer $Kd = 3$ μM [25, 26]. This led us to hypothesize that the full-length IL-2Rβ chain might also exist as a homodimeric molecule.

In the work presented here, we first analyzed the ability of full length IL-2Rβ chains to form dimers. In the same manner as for IL-2Rβ/γc heterodimers, we observed that IL-2Rβ/β homodimers assemble spontaneously at the cell surface, even in the absence of the cytokine. We then studied IL-2 binding to cells expressing IL-2Rβ only. It was seen that the heterodimers and homodimers have similar intermediate affinities for IL-2. Our results show that IL-2Rβ subunits form homodimers binding IL-2; they may represent a new form of the IL-2R.

METHODS AND MATERIALS

Cell lines

Green monkey kidney fibroblast cells (COS-7 line) and human embryonic kidney cells (HEK-293), which do not express any of the IL-2R chains, were used in transient transfection experiments. The IL-2-dependent human CD4 T cell line Kit-225 constitutively expresses IL-2Rα, IL-2Rβ and γc chains [27].

COS-7 cell transfection with plasmids coding for HA- and MYC-tagged IL-2Rβ and γc chains

Human genes for IL-2Rβ and γc from T lymphocyte cDNA were amplified by standard PCR. dsDNA fragments were cleaved and subcloned in the plasmid pcDNA (Invitrogen, Carlsbad, CA, USA). Fusions of HA and MYC tags at the C-terminus were constructed by subcloning IL-2Rβ and γc coding sequences using PCR and restriction enzyme digestion within BamHI/EcoRI cloning sites of pcDNA-HA and pEF6-MYC:His_6 (Invitrogen). Oligonucleotides were synthesized by Proligo-France (Paris).

COS-7 cell transfections were performed in 6-well culture plates (2.10^5 cells/2 mL well) with 0.5 μg of pcDNA plasmids coding for either IL-2Rβ:HA, IL-2Rβ:MYC or γc:MYC, or various combinations of these, and JetPEI transfection reagent (Qbiogene, Illkirch, France) according to the manufacturer's instructions (2 μg of dsDNA, 4 μL JetPEI, 2 mL media). Incubation for 48 h at 37°C gave the most efficient transfection yields. When indicated, COS-7 cells were incubated for 1 hour at 37°C with increasing concentrations of IL-2, from 1 to 100 nM, before harvesting.

Immunoprecipitation and Western blot of HA- and MYC-tagged chains

Cells were harvested and treated for 20 min on ice with lysis buffer consisting of 0.5% Triton-X100, 50 mM Tris-HCl, 150 mM NaCl, 1mM EDTA, 1mM EGTA, 10 μg/mL PMSF, 1 mM sodium orthovanadate, 10 μg/mL leupeptin and 1 μg/mL aprotinin. Transfected COS-7 cell lysates containing about 200 μg of protein were incubated with 7.5 μL of anti-HA (mouse IgG2b, clone 12CA5, Roche, Basel, Switzerland) or anti-MYC antibodies (mouse IgG1, clone 9E10, SCB, Santa Cruz Biotechnology, CA, US) for 2 hours at 4°C with agitation. G-protein-coupled sepharose beads (Amersham-GE Healthcare, Piscataway, NJ, USA) were then added for 1 h at 4°C. After 4 washes in 0.5% Triton-X100 buffer, samples were denatured for 5 min at 100°C in SDS-loading buffer (62.5 mM Tris-HCl, 10% glycerol, 2% SDS and bromophenol blue) and 5% 2-mercaptoethanol. Proteins were separated by electrophoresis on an 8.5% SDS-polyacrylamide gel (SDS-PAGE) and transferred onto a polyvinylidine difluoride membrane (PVDF; Millipore, Bedford, MA, USA) overnight at 4°C. The membrane was saturated with milk, incubated with anti-HA or anti-MYC antibodies (2 hours) and washed in TBS 0.5% Tween-20 buffer before being incubated with HRP-coupled anti-mouse antibody (Amersham). Proteins were revealed by ECL Western blotting detection reagents (Amersham).

Förster resonance energy transfer (FRET) between IL-2Rβ:ECFP and IL-2Rβ:EYFP at the surface of transfected COS-7 cell measured by confocal microscopy

Human IL-2Rβ and γc cDNAs were cloned in HindIII/KpnI sites of pECFP, pEGFP, pEYFP plasmids (BD-Biosciences, Bedford, MA, USA), upstream of EGFP, ECFP or EYFP gene sequences derived from GFP, optimised for fluorescence properties and the absence of dimerization. The peptide linker EFCSRRYRGPGIHRPVAT was used as a hinge between the two unmodified sequences of the receptor and EXFP domains. IL-2Rβ (UNIPROT ID. P14784, European Bioinformatics Institute) and γc (UNIPROT ID. P31795) are composed of a signal peptide (residues 1-26 and 1-22), an amino terminal extracellular domain (27-240 and 23-262), a single transmembrane domain (241-265 and 263-283) and a carboxy terminal cytoplamic domain (266-551 and 284-369). Several constructs of IL-2Rβ fragments coding for the receptor chain, and consisting of the sequence signal without the cytoplasmic domain (1-272) or without the extracytoplasmic domain (1-33, 230-551), were fused to ECFP and EYFP. Corresponding constructions were also obtained for the γc chain coding for residues 1-283 and 1-39, 249-369. The sequences of all constructions were verified (Genome Express, Maylan, France).

COS-7 cells growing over 22 mm cover slides in 6-well plates were transiently transfected with one or a combination of plasmids, as indicated. After 48 h, the cells were washed with 5 mL PBS-0.02% azide then fixed in 1% paraformaldehyde (PFA) and mounted using Vectashield medium (Vector Laboratories, Burlingame, CA, USA). Unfixed COS cells were also observed: transfected cells were grown in glass-bottom dishes (Matek, Ashland, MA) in colourless RPMI medium (Cambrex). Images of COS-7 cells were obtained by means of a laser scanning Meta Zeiss confocal microscope (Carl Zeiss S.A.S., Le Pecq, France) through a plan-apochromat x63/1.4 (oil DIC)

Zeiss objective. Images were analyzed at room temperature and processed by LSM 510 software (Carl Zeiss). ECFP, EGFP and EYFP fluorescences were observed using the following excitation/emission wavelengths: 458 nm/480-530 nm, 514 nm/535-580 nm, 514 nm/535-580 nm [28-30]. FRET was measured from ECFP donor excitation at 458nm and EYFP emission measurements between 535-580 nm. FRET efficiency was measured by irradiating EYFP energy acceptors at 514 nm in a square selected on the cell surface then comparing ECFP fluorescence emission intensity in the corresponding square before and after EYFP irradiation [29, 30]. The distance *R* between ECFP and EYFP fluorescence centers was extrapolated from the ratio of ECFP fluorescence intensities before (I_{ECFP}) and after EYFP irradiation (I^*_{ECFP}) in accordance with the Förster definition [30].

IL-2-biotin binding assays on HEK-293 cells transfected with plasmid coding for IL-2Rβ:EGFP

Binding of biotinylated IL-2 was assayed by FACS at the surface of transiently transfected HEK-293 cells expressing IL-2Rβ:EGFP using the same transfection protocol as described above for COS-7 cells. Various amounts of IL-2-biotin (R and D Systems, Minneapolis, MN, USA), from 0-100 nM were added to 5.10^5 of transfected HEK-293 cells suspended in 200 µL of PBS-BSA (3 mg/mL) and incubated on ice for 30 min. Streptavidin-alexafluor 633 (SA633; 0.5 µg/mL; Invitrogen) was then added and the cells maintained at 4°C for 15 min. When indicated, anti-IL-2Rβ monoclonal antibodies (mouse, clone A41, kindly provided by Dr. Y. Jacques, INSERM, Nantes, France) or control anti-mouse IL-4 monoclonal antibodies (rat IgG1, clone 11B11, kindly provided by Dr W. Paul, NIH, Bethesda, MD, USA) were added and then maintained on ice for 30 min prior to IL-2-biotin exposure. The preparation was washed three times with 2 mL of RDF1 washing buffer. The cells were finally resuspended in 250 µL and kept on ice pending flow cytometry analysis. Kit-225 cells were used as positive controls and untransfected HEK-293 cells as negative controls. Flow cytometry analyses were performed on 40 000 positive counts (FACScalibur; Becton Dickinson, Mountain View, CA, USA).

^{125}I-labeled IL-2 binding assays

IL-2 as 100 µL of a 1 µg/mL (59 µM) solution (Chiron-Novartis, Basel, Switzerland) in 100 mM sodium phosphate buffer was labelled with 10 µL of ^{125}I (0.5 mCi; MP Biomedicals, Illkirch, France) using the chloramine T method (7.5 µg chloramine T; Riedel-de Haën, Seelze, Germany), to a specific activity of 734.10^6 cpm/mg. The iodination reaction was stopped with 50 µL of Tyr-saturated aqueous solution. IL-2 was separated from ^{125}I and Tyr on a Sephadex G-25 column (5 mL) with collection of 40 µL fractions. A set of ^{125}I-labeled IL-2 binding curves and corresponding Scatchard plots were constructed as described elsewhere [31]. Cells were counted twice on a Beckman-Coulter Z2 (Fullerton, CA, USA). Binding experiments were conducted at 4°C on 2-10 million cells suspended for 60 min in a solution containing PBS, 0.02% sodium azide and a BSA concentration of 5 mg/mL in the presence of various amounts of ^{125}I-labeled IL-2; the total volume was 80 µL per sample. A 100-fold molar excess of cold IL-2 was added for 10 min at 4°C followed by 2 mL of cold PBS, 0.02% sodium azide and BSA 10 mg/mL solution. Cells were then vortexed briefly before being centrifuged for 5 min at 3000 rpm. Cell and supernatant radioactivity was measured twice for 1 min on a multi-crystal LB 2111 gamma counter supplied by Berthold Technologies (Bad Wildbad, Germany) and analyzed by Lbis software. *Kd* values and the number of binding sites were obtained by fitting the binding curves using Origin 6.0 software (Microcal, Northampton, MA, USA) and the results were displayed as Scatchard plots for convenience [31].

RESULTS

IL-2Rβ chains form dimers in the absence of IL-2

Our previous experiments demonstrated that the soluble ectodomain in IL-2Rβ (residues 31-200) dimerizes spontaneously in solution [25, 26]. To confirm and further extend this finding, we undertook to analyze the association of full-length IL-2Rβ chains at the cell surface. COS-7 cells were transiently transfected by plasmids coding for IL-2Rβ tagged with either HA or MYC epitopes, and when indicated were cotransfected with both plasmids. The transfected cells were lysed and the receptor chains immunoprecipitated by anti-HA antibodies (*figure 1A* and *B*). The complexes were separated by SDS-PAGE and analyzed by Western blot using anti-HA *(figure 1A)* or anti-MYC antibodies *(figure 1B)*. When the cells were cotransfected with both plasmids, anti-HA immunoprecipitation pulled down the IL-2Rβ:HA/IL-2Rβ:MYC complex, which was then detected by anti-MYC antibodies *(figure 1B)*. Cell lysates were also immunoprecipitated by anti-MYC antibodies (*figure 1C* and *D*). Western blots with anti-HA also showed a band when the cells were transfected with both plasmids *(figure 1C)*. The γc:MYC fusion was used as a control *(figure 1D)*. Anti-HA immunoprecipitation also pulled down the IL-2Rβ:HA/γc:MYC complex when COS-7 cells were transfected with both plasmids as shown by anti-MYC detection of γc:MYC from this complex *(figure 1D)*. The reverse procedure was also investigated: anti-MYC immunoprecipitation of the same complex enabling anti-HA detection of IL-2Rβ:HA *(figure 1C)*.

Additional experiments were performed to verify the specificity of IL-2Rβ dimerization *(figure 2)*. When lysates from two separate COS-7 cell preparations were mixed, i.e. one transfected by IL-2Rβ:HA and the other by IL-2Rβ:MYC, no coimmunoprecipitation was observed. This indicates that no IL-2Rβ:HA/IL-2Rβ:MYC dimers were formed during the lysis or precipitation procedures. The MW of the IL-2Rβ:HA/IL-2Rβ:MYC complex was determined under both reducing and non-reducing conditions. Our observations indicate that the IL-2Rβ:HA/IL-2Rβ:MYC association does not involve any intermolecular disulfide bridges. Furthermore, the specificity of the coimmunoprecipitation was verified using various control-tagged proteins expressed after co-transfection with IL-2Rβ:HA.

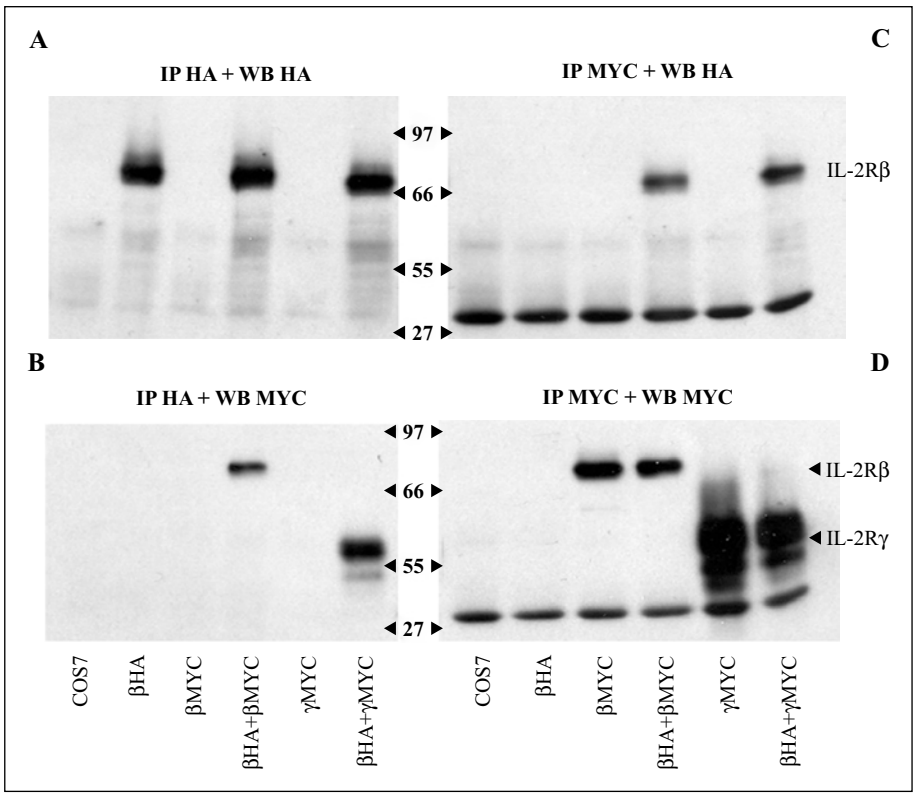

Figure 1
IL-2Rβ:HA/IL-2Rβ:MYC and IL-2Rβ:HA/γc: MYC association in COS-7 transfected cells.
COS-7 cells were transfected with pcDNA vectors prepared as described in Methods and materials. pcDNA-IL-2Rβ:HA or pcDNA-IL-2Rβ:MYC were used alone or in combination. Cell lysates were immunoprecipitated by anti-HA (**A** and **B**) or anti-MYC (**C** and **D**) antibodies and analyzed by Western blotting using anti-HA (**A** and **C**) or anti-MYC (**B** and **D**) reagents.

IL-2Rβ homodimerization is inhibited by γc and slightly favored by IL-2

In order to characterize the binding preference of the IL-2Rβ chain either to itself or to γc, COS-7 cells were transfected by three plasmids coding for IL-2Rβ:HA, IL-2Rβ:MYC and γc:MYC. As expected, IL-2Rβ dimer formation was decreased by the presence of γc chains, with competition clearly taking place between IL-2Rβ:MYC and γc:MYC for binding to IL-2Rβ:HA. The Western blot *(figure 3)* showed a faint band for IL-2Rβ:MYC and an intense band for γc:MYC, indicating that IL-2Rβ has greater affinity for γc than for itself. This competition also suggests that IL-2Rβ chains mainly form dimers, and not heavier oligomers.

The effect of IL-2 on dimer formation was also investigated. Here, COS-7 cells transfected with plasmid pairs coding for IL-2Rβ:HA/IL-2Rβ:MYC and for IL-2Rβ:HA/γc:MYC were incubated for 1 hour with 0, 10 and 100 nM of IL-2 before the preparation of lysates *(figure 3)*. These were immunoprecipitated by anti-HA and blotted with anti-MYC antibodies. A slight but reproducible IL-2 effect on both IL-2Rβ:HA/IL-2Rβ:MYC and IL-2Rβ:HA/γc:MYC complex formation was observed with a maximum effect at about 10 nM. Overall, these experiments, which were repeated three times, confirmed that IL-2 is not required for the assembly of IL-2Rβ/β dimers and suggested that the cytokine may bind IL-2Rβ/β dimers directly and stabilize them.

FRET analysis of IL-2Rβ homodimer assembly at the surface of COS-7 cells

Immunoprecipitation experiments were conducted on lysed cells. Thus, to confirm further the observation of dimer formation at the surface of living cells, we measured the specific FRET between IL-2Rβ chimeras fused to GFP derivatives. To do this, COS-7 cells were transfected with plasmids coding for the IL-2Rβ:ECFP and IL-2Rβ:EYFP constructs. We checked the specificity of the FRET from the donor (ECFP) to the acceptor (EYFP) by comparing FRET and fluorescence intensities from donors and acceptors before and after acceptor irradiation. Thus, ten measurements of ECFP, EYFP and FRET fluorescence intensities were acquired by confocal microscopy in the course of 4-min kinetics on two, square regions designated 1 and 2 *(figure 4A)* at the surface of PFA-fixed COS cells. The first three points gave an indication of the photobleaching drift. We then irradiated EYFP for one minute in the square region 1. We then measured ECFP, EYFP and FRET fluorescence intensities for the next two minutes in both regions 1 (irradiated) and 2 (non-irradiated). The intensity of the fluorescence emitted by the donor ECFP increased after irradiation of the EYFP acceptor in square region 1 in comparison with non-irradiated control square region 2 *(figure 4B)*. This process was repeated 10 times on different cells in the same preparation presenting roughly the same fluorescence intensities from ECFP (± 15%) and from EYFP (± 15%) in the same square area. Acceptor

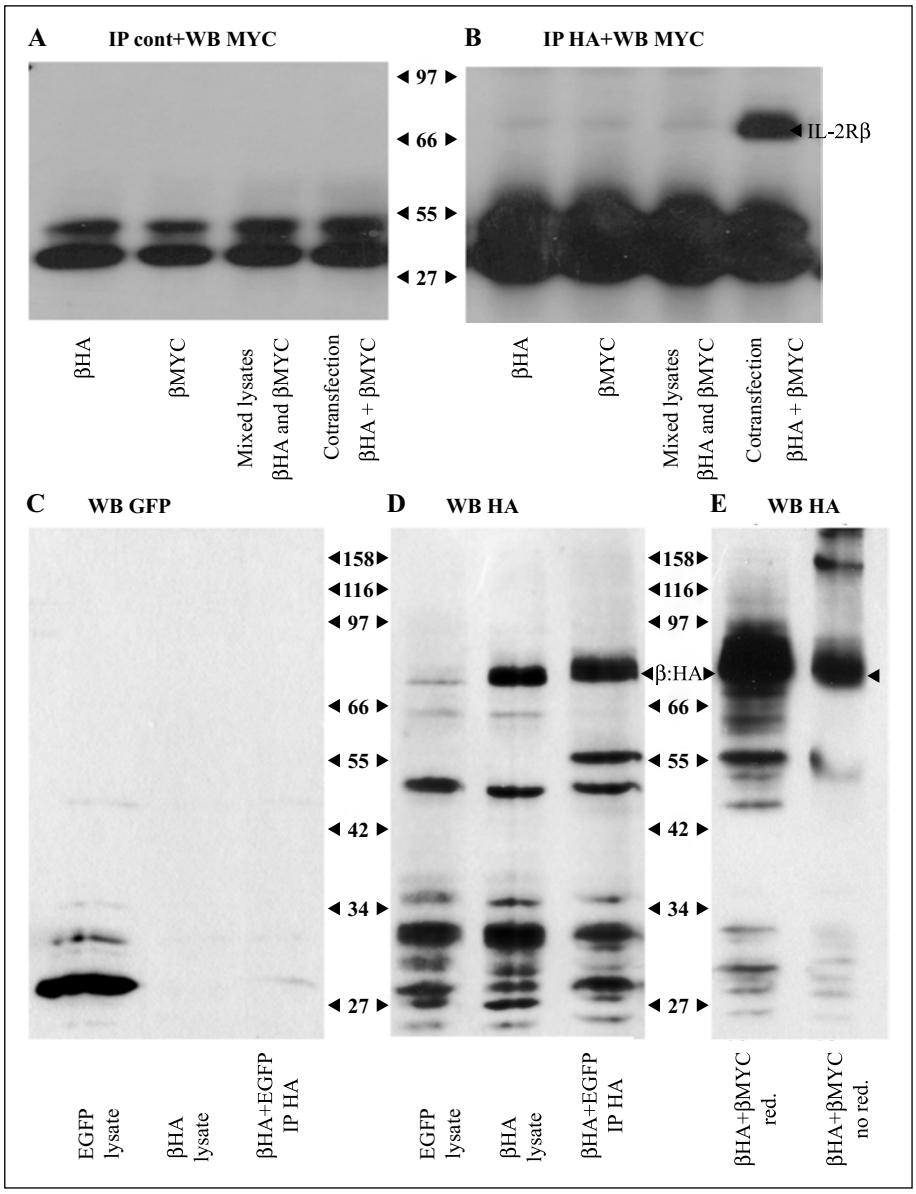

Figure 2

Specificity of IL-2Rβ homodimerization in transfected COS-7 cells.

A, B) Cell lysates were prepared from COS-7 cells transfected by a single plasmid and when indicated, cell lysates from two separate preparations of single-plasmid-transfected cells were mixed together (IL-2Rβ:HA and IL-2Rβ:MYC). Lysates were also prepared using cells co-transfected with both plasmids (IL-2Rβ:HA + IL-2Rβ:MYC). The lysates were immunoprecipitated with control antibodies (**A**) or anti-HA antibodies (**B**) and migrated in SDS-PAGE. Western blotting was performed with anti-MYC antibodies.

C, D) COS-7 cells were transfected with pBD-EGFP or pcDNA-IL-2Rβ:HA. Cell lysates were migrated in SDS-PAGE. COS-7 cells were also transfected with pBD-EGFP and pcDNA-IL-2Rβ:HA and cell lysates immunoprecipitated with anti-HA antibodies prior to analysis in SDS-PAGE. Western blotting was performed with anti-GFP (**C**) or anti-HA antibodies (**D**).

E) COS-7 cells were transfected with pcDNA-IL-2Rβ:HA and pcDNA-IL-2Rβ:MYC vectors. Lysates were immunoprecipitated with anti-MYC. Before migration, the samples prepared in SDS-loading buffer were heated in the presence of 2-mercaptoethanol (red. = reducing condition) or in the absence of 2-mercaptoethanol (no red). Western blotting was performed with anti-HA antibodies.

irradiation disrupted specific energy transfers not only in the high intensity regions *(table 1A)* and in darker regions (membrane observed vertical to the nucleus, *table 1B*) of highly transfected cells, but also in very low-transfected cells, with 50 times less ECFP and EYFP fluorescence *(table 1C)*. When FRET efficiency $E^{\%}$ exceeded 3%, we considered that the FRET intensity was due to the proximity of ECFP and EYFP fluorescent domains in the same complex, not neighbouring complexes [28-30]. We verified that ECFP and EYFP did not contribute to the binding of chimeras and that no FRET occurred between unassociated pairs; FRET efficiency values $E^{\%}$ for the ECFP and EYFP pairs expressed together in transfected COS cytoplasm were less than 3% (Förster distance $R > 90$ Å; *table 1*). FRET efficiencies and corresponding chimera pairs are described in *figure 4C-E*. Calculated Förster distances *R,* correspond to averaged distance values between X:ECFP/Y:EYFP pairs contributing to FRET. FRET efficiencies and *R* values are detailed in *table 1*. When COS-7 were transfected with plasmid pairs, the distance between IL-2Rβ:ECFP and IL-2Rβ:EYFP ($R < 69.8$ Å ± 2.2) was found to be the same as the distance between the IL-2Rβ:ECFP and γc:EYFP pair ($R < 70.3$ Å ± 2.3). In both cases, we characterized spe-

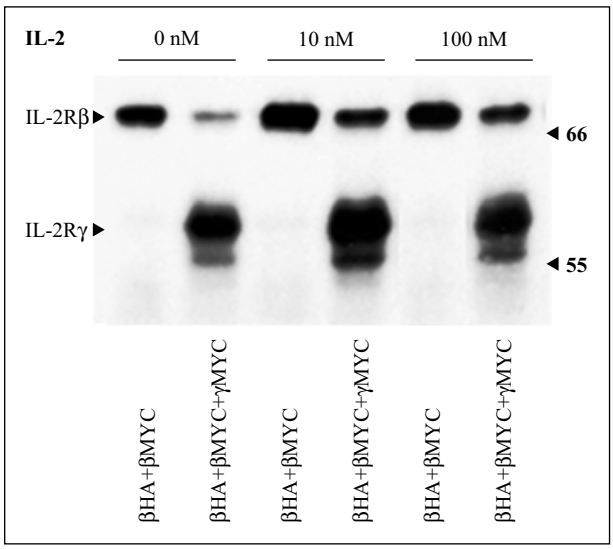

Figure 3
Competition for IL-2Rβ/β and IL-2Rβ/γc dimer formation in COS-7 transfected cells.
COS-7 cells were transfected by both pcDNA-IL-2Rβ:HA and pcDNA-IL-2Rβ:MYC or the three pcDNA-IL-2Rβ:HA, pcDNA-IL-2Rβ:MYC and pcDNA-γc:MYC plasmids. When indicated, the cells were incubated before lysis for 15 minutes with the indicated amounts of IL-2. Protein complexes were precipitated by anti-HA, separated by SDS-PAGE and blotted with anti-MYC antibodies.

cific FRET as an indication of the physical interaction between IL-2R chains.

We also measured FRET from various combinations of IL-2Rβ:ECFP and IL-2Rβ:EYFP constructs lacking external or internal domains in order to locate the critical region involved in receptor homodimerization and confirm that FRET results were from binding and not from chain crowding. The distance between receptor chains lacking the IL-2R$\beta_{27–272}$:ECFP and IL-2R$\beta_{27–272}$:EYFP ($R < 63.5$ Å ± 2.1) cytoplasmic domains was similar to that noted for the IL-2Rβ:ECFP and IL-2Rβ:EYFP full chains whereas no FRET was measured between receptor chains lacking the IL-2R$\beta_{230–551}$:ECFP and IL-2R$\beta_{230–551}$:EYFP extracellular domains ($R > 90$ Å). These results demonstrate that ectodomains are able to interact with one another at the cell surface in the absence of other factors, as described in sedimentation experiments. Conversely, the cytoplasmic and transmembrane domains did not contribute significantly to homodimerization. The IL-2R$\beta_{230–551}$:ECFP and IL-2R$\beta_{230–551}$:EYFP pair was considered as a negative control for the FRET experiments. We also used co-expressed IL-2Rβ:ECFP with cytoplasmic EYFP and IL-2Rβ:EYFP with cytoplasmic ECFP as negative controls: no FRET was observed in either case. These experiments were repeated using unfixed COS cells in glass-bottomed dishes. Fluorescence intensities were far lower and more sensitive to bleaching in the absence of protective mounting medium, making the experiments more difficult to perform. Thus, FRET efficiencies measured on ten cells were roughly the same as those calculated from PFA-fixed cells with larger standard errors: $E^{\%} = 11\% \pm 6$; $R < 71$ Å ± 7 for the IL-2Rβ:ECFP/IL-2Rβ:EYFP pair and $E^{\%} = 16\% \pm 8$; $R < 66$ Å ± 9 for the IL-2Rβ:ECFP/γc:EYFP pair. These experiments confirmed that IL-2Rβ/β homodimers are present at the surface of living cells even in the absence of cytokine and clearly demonstrated the involvement of IL-2Rβ extracellular domains in IL-2Rβ homodimerization.

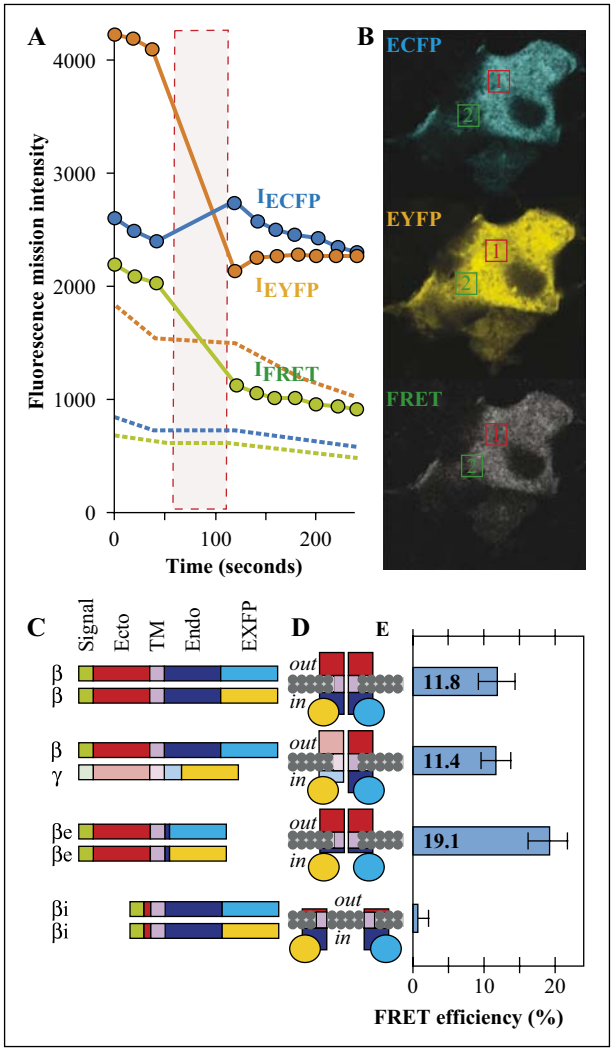

Figure 4
FRET from IL-2Rβ:ECFP to IL-2Rβ:EYFP expressed by transfected COS-7 cells.
A) COS-7 cells were co-transfected by pBD-IL-2Rβ:ECFP and pBD-IL-2Rβ:EYFP plasmids. Fluorescence intensities I_{ECFP}, I_{EYFP}, I_{FRET} for ECFP, EYFP and FRET respectively, recorded in square regions 1 and 2 as indicated in the cell pictures, are plotted against time on the left graph as solid (irradiated region 1) and dashed lines (non-irradiated region 2), over the 4 min kinetics experiment. 514 nm irradiation for 1 min of region 1 is indicated as a red stripe on the graph. **B**) Pictures corresponding to the three fluorescence channels at the end point (240 sec) are reported on the right. **C**) Receptor: EXFP-gene constructions expressed in COS-7 cells then tested by this procedure are detailed as colored boxes: signal peptide (signal), extracellular (ecto), transmembrane (TM) and cytoplasmic (endo) domains, ECFP and EYFP (cyan and yellow boxes). Hypothesis of their corresponding protein assembly are schematized in **D**), embedded in the membrane. **E**) FRET efficiencies are reported as horizontal blue bars with black errors bars on their tips. Corresponding relative fluorescence intensities and Förster distances from chimera pairs are reported in *table 1*.

IL-2 binds specifically to the IL-2Rβ chain at the surface of transfected COS-7 and HEK-293 cells

Our previous results suggested that IL-2 might bind IL-2Rβ/β dimers. We used FACS to assay the binding of IL-2-biotin to HEK-293 cells transfected with plasmid

Table 1
FRET measurements between IL-2R subunits

A					
Donnor **Acceptor**	**[a]β:ECFP** **β:EYFP**	**[b]β:ECFP** **β:EYFP**	**[c]β:ECFP** **β:EYFP**	**[d]βe:ECFP** **βe:EYFP**	**[e]βi:ECFP** **βi:EYFP**
I_{ECFP}	2450	570	45	1 672	105
I_{FRET}/I_{ECFP}	0.82	0.79	0.70	0.82	0.31
I_{FRET}/I_{EYFP}	0.49	0.43	0.47	0.63	0.22
I^*_{FRET}/I_{FRET}	0.57	0.71	0.78	0.44	0.88
E %	11.8 ± 2	8.79 ± 3	6.03 ± 2	19.14 ± 3	0.58 ± 2
$R_{Förster}$	70Å ± 2	73Å ± 4	79Å ± 4	63Å ± 2	117Å ± 13
B					
Donnor **Acceptor**	**[f]β:ECFP** **γ:EYFP**	**[g]γ:ECFP** **γ:EYFP**	**[h]β:ECFP** **EYFP**	**[i]ECFP** **β:EYFP**	**[j]ECFP** **EYFP**
I_{ECFP}	2 590	1 660	2 250	2 650	2 870
I_{FRET}/I_{ECFP}	0.82	0.33	0.44	0.44	0.43
I_{FRET}/I_{EYFP}	0.49	0.19	0.24	0.27	0.27
I^*_{FRET}/I_{FRET}	0.54	0.86	0.88	0.85	0.88
E %	11.4 ± 2	0.91 ± 2	0.36 ± 2	0.33 ± 2	0.23 ± 2
$R_{Förster}$	70Å ± 2	109Å ± 9	127 ± 17	129 ± 18	137 ± 22

COS-7 cells were transiently co-transfected to express chimera pairs detailed in each column. I_{ECFP} fluorescence intensity from ECFP, I_{FRET}/I_{ECFP} and I_{FRET}/I_{EYFP} values from FRET / ECFP (donor) and for FRET / EYFP (acceptor) fluorescence intensity ratios measured in region 1 in the absence of IL-2 are reported from a representative experiment out of ten. Ratios for FRET intensities after (I^*_{FRET}) and before irradiation (I_{FRET}) are also reported. FRET efficiency $E^{\%} = 100\% \times (I^*_{ECFP} - I_{ECFP})/I^*_{ECFP}$ is reported as a percentage with the standard error for ten experiments from ECFP intensity before (I_{ECFP}) and after irradiation (I^*_{ECFP}). Corresponding distances and errors are indicated according to $R = R_0\,[1\text{-}1/(I^*_{ECFP} / I_{ECFP})]^{1/6}$, where $R_0 = 50$ Å. FRET from COS transfected with IL-2Rβ:ECFP/ IL-2Rβ:EYFP was measured in high-expression cells in a region above the cytoplasm encompassing vesicles (a), and in a region above the nucleus devoid of vesicles (b) then in cells with 50-times lower expression of IL-2Rβ:ECFP and IL-2Rβ:EYFP (c). FRET was also measured between the constructs IL-2Rβe:ECFP/βe:EYFP (d) and IL-2Rβi:ECFP/βi:EYFP (e) where IL-2Rβ*e* is the subunit deprived of the cytoplasmic domain (β27-272:EXFP) and IL-2Rβ*i* is the subunit deprived of the ectodomain (β230-551:EXFP). The lower table shows all the following controls: the heterodimeric complex IL-2Rβ:ECFP/γc:EYFP (f) and the non-associative pairs γc:ECFP/γc:EYFP (g), IL-2Rβ:ECFP/EYFP (h), ECFP/ IL-2Rβ:EYFP (i) and ECFP/EYFP (j).

expressing the IL-2Rβ:EGFP fusion. Binding experiments using various amounts of IL-2–biotin in the range 10 pM-100 nM were repeated three times on transfected HEK-293 cells. Transfection efficiency exceeded 70% according to the fluorescence of the IL-2Rβ:EGFP chimera expressed by cells analyzed by FACS. One representative experiment out of three is shown in *figure 5A*. Saturation was reached at concentrations above 2 nM IL-2, with a plateau up to 10 nM, and 50% maximum IL-2-biotin binding was obtained from 0.7 to 1.2 nM. *Figure 5B* also shows that this binding was specifically inhibited by anti-IL-2Rβ mAb (A-41), but not by anti-mIL4 (11B11) mAb used as control.

Equilibrium dissociation constants for ^{125}I-labeled IL-2 were measured at 4°C at the surface of transiently transfected COS-7 cells expressing either IL-2Rβ alone, γc alone or both chains. *Kd* and the number of binding sites were computed from the best fit with the saturation curve, plotting cell-bound ^{125}I-labeled IL-2 against free ^{125}I-labeled IL-2. The corresponding Scatchard plots are presented in *figure 6*. The control Kit cells expressing IL-2Rα, IL-2Rβ and γc chains showed three species of binding sites characterized by high affinity (*Kd* = 13 pM ± 3, 210 sites), intermediate affinity (*Kd* = 0.9 nM ± 0.2, 4 340 sites) and low affinity (*Kd* = 19 nM ± 4, 135 500 sites) properties. Transfected COS cells expressing the IL-2Rβ chain but not γc, bound IL-2 with two species of binding sites characterized by intermediate (*Kd* = 1.0 nM ± 0.2, 11 240 sites) and low (*Kd* = 172 nM ± 25, 23 400 sites) affinities that might correspond to IL-2Rβ homodimers and monomers, respectively. Transfected COS-7 cells expressing IL-2Rβ and γc also showed intermediate affinity (0.9 nM ± 0.2, 17 860 sites; data not shown) suggesting that IL-2Rβ/β ho-

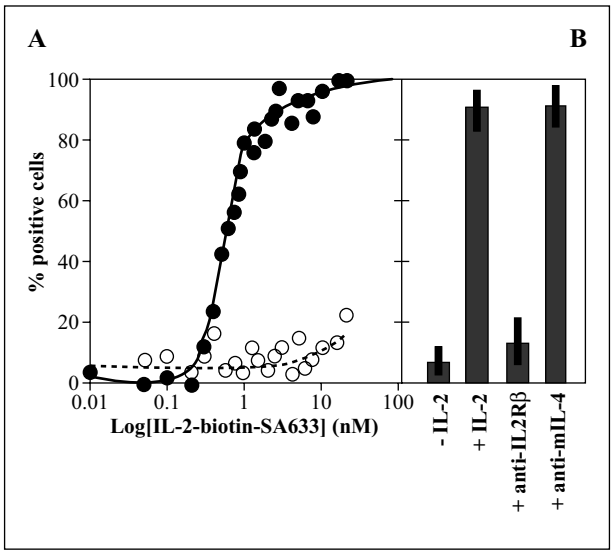

Figure 5
IL-2-biotin binding assays at the surface of transfected HEK-293 cells expressing IL-2Rβ:EGFP.
A) Binding of IL-2-biotin (0-20 nM), detected by SA633, was analysed by FACS at the surface of HEK-293 cells transfected by pBD-IL-2Rβ:EGFP. Cells expressing IL-2Rβ:EGFP were analyzed and the percentage of cells binding IL-2–biotin–SA633 is plotted (closed circles) against IL-2 concentration (log scale). The lack of any IL-2 binding by non-transfected cells is also shown (open circles).
B) Inhibition of IL-2-biotin-SA633 (2nM) binding was analyzed by FACS at the surface of HEK-293 cells. The percentage inhibition by pre-incubation with anti-IL-2Rβ mAb is reported. The lack of any inhibition by control mAb (anti-mIL4:11B11) is also shown. The mAb were used at 1 μg/mL final concentration.

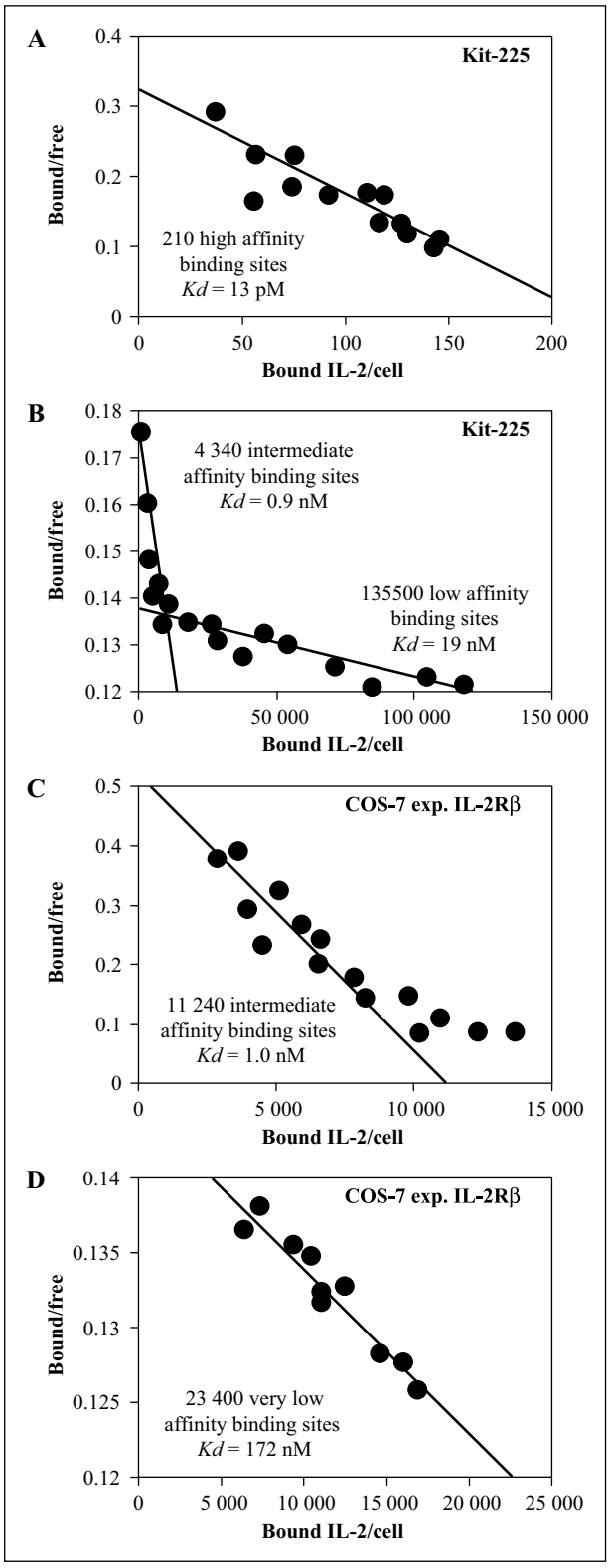

Figure 6
^{125}I-labeled IL-2 binding at the surface of Kit-225 and COS-7 cells expressing IL-2Rβ.
Scatchard plots of ^{125}I-labeled IL-2 binding to Kit (**A, B**) and transfected COS-7 cells by IL-2Rβ (**C, D**). Various amounts of ^{125}I-labeled IL-2 were added to 1-10 million cells in 80 µL of PBS sodium azide buffer for 60 min at 4°C giving up to 36 concentrations in the range 10 pM-1 µM. 100-fold molar excess of cold buffer was added for 10 min before a short washing step and 5 min centrifugation. ^{125}I-labeled IL-2 binding curves were fitted to the corresponding *Kd* values and shown in the corresponding panels.

modimers and IL-2Rβ/γc heterodimers have similar affinities for IL-2 at the surface of COS-7 cells. Under the same conditions, IL-2 concentrations below 100 nM did not produce any significant binding on the surface of transfected COS-7 cells expressing γc or on the surface of untransfected COS-7 cells used as controls (data not shown). These experiments demonstrated that IL-2 binds with intermediate affinity to cells expressing IL-2Rβ in the absence of IL-2Rα and γc, which are not expressed in COS-7 cells.

DISCUSSION

The components of the IL-2R were identified and described more than a decade ago, but the mechanism and genesis of the receptor assembly at the cell surface remains elusive. The structure of the complex formed between three IL-2Rα, IL-2Rβ and γc ectodomains and IL-2 has been elucidated [22, 23], and an exhaustive microcalorimetric study has shown that the soluble IL-2Rβ and γc fragments have very low affinity one for the other and may associate *via* IL-2 [24]. We previously described the propensity of the IL-2Rβ ectodomain to homodimerize *in vitro* with very low affinity in the absence of IL-2 [24, 25]. In the work described here, we extended the relevance of this observation at the cell surface, suggesting that the affinity between IL-2Rβ chains embedded in the membrane is substantially increased. We showed that full-length IL-2Rβ dimerizes spontaneously in the absence of cytokine at the surface of cells that do not express γc chains, forming a receptor able to induce protein phosphorylation upon IL-2 binding. This observation may have important immunological relevance for the lymphocyte subpopulations that present at their surface an excess of IL-2Rβ over γc as described for NK cells [32].
We used two distinct approaches, with COS-7 cells expressing IL-2Rβ to demonstrate the existence of IL-2Rβ/β homodimers at the cell surface in the absence of IL-2. Firstly, coimmunoprecipitation of IL-2Rβ:HA/IL-2Rβ:MYC demonstrated that IL-2Rβ chains oligomerize. We showed that oligomerization is not a direct consequence of IL-2Rβ over-production and does not require the formation of intermolecular disulfide bridges. Secondly, we detected specific FRET between IL-2Rβ:ECFP/IL-2Rβ:EYFP, proving that homodimerization is observable at the surface of living cells. We also observed coimmunoprecipitation between IL-2Rβ:HA/γc:MYC and FRET and between IL-2Rβ:ECFP/γc:EYFP in the absence of IL-2. These results confirm the FRET measurements between IL-2Rβ and γc labeled by FITC- and Cy3-mAbs and analysed by FACS, suggesting that the IL-2Rβ/γc heterodimer is also formed prior to cytokine binding [33]. Finally, we demonstrated by coimmunoprecipitation that IL-2Rβ competes with γc for the formation of dimers. IL-2Rβ/γc heterodimers are strongly favored over IL-2Rβ/β homodimers since IL-2Rβ has a higher affinity for γc than for itself. These observations suggest that IL-2Rβ/β homodimers are formed only when the IL-2Rβ chain is expressed in excess of the γc chain. Earlier studies did not conclude that IL-2Rβ/γc and IL-2Rβ/β complexes are formed in transfected COS-7, HeLa or MOLT4 cells by coimmunoprecipitation in the absence of cytokine [34]. We suggest that the complex was detected only after IL-2 exposure because receptor chain expression was low and

the cytokine stabilizes the low-expressed complex in agreement with *figure 2*. We used more potent promoters for IL-2Rβ and γc gene expression in plasmids; chain concentration in transfected cell was not then limiting complex formation in the absence of cytokine at a level comparable to what is observed in the Kit-225 human T lymphocyte cell line [33]. Thus, the number of IL-2R complexes is in the same order of magnitude in transfected COS cells as in Kit-225 cells. Moreover, our experimental approach using HA- and MYC-tagged proteins is particularly sensitive for detecting interactions in cell lysates.

IL-2Rβ and γc possess similar putative domain architectures: an N-terminal ectodomain connected by a single transmembrane helix to a C-terminal endodomain. The cytoplasmic domain of the γc chain is rather small (86 residues), whereas the corresponding domain in the IL-2Rβ chain is larger and contains 286 residues. By contrast, the ectodomains in the IL-2Rβ and γc chains show similar features. We have already shown by analytical ultracentrifugation that the IL-2Rβ ectodomain (residues 31-230) dimerizes spontaneously in solution. We have showed here, in this study, that deletions from the IL-2Rβ cytoplasmic domain did not alter FRET between IL-2Rβ:ECFP and IL-2Rβ:EYFP molecules at the COS-7 cell surface. Conversely, no FRET was observed when the IL-2Rβ ectodomain was deleted in the full chain: ectodomain and transmembrane domains may contribute, but are not required for homodimerization. We concluded that ectodomain interactions control homodimer formation by full-length IL-2Rβ molecules and enable IL-2 binding with significant affinity. Furthermore, IL-2 binds to IL-2Rβ and stabilizes the dimers. It is noteworthy that the homodimer association constant is increased by several orders of magnitude when affinity for free diffusible molecules in solution (three-dimensional motions) is converted to pre-oriented (inside-outside) and pre-aligned molecules embedded in the same membrane (slower two-dimensional motions).

The question of IL-2 binding to IL-2Rβ chains warrants discussion. Several studies have shown that IL-2 is able to bind to soluble IL-2Rβ monomers, although with low affinity (*Kd* from 144 to 534 nM) [24, 35] and our work also suggests that the IL-2Rβ monomer undergoes this low affinity binding at the cell surface (*Kd* = 172 nM). We have ourselves reported on the ability of the IL-2Rβ ectodomain to dimerize and bind the IL-2 mimetic, P1-30, as measured by analytical ultracentrifugation [25, 26]. Here, we have developed a new approach to reinvestigate this point. Using confocal microscopy, we show that COS-7 cells are able to bind IL-2 after transfection with IL-2Rβ:EGFP constructs. This approach was extended to FACS analysis of HEK-293 cells transfected with IL-2Rβ:EGFP constructs. This experimental approach was therefore used to quantify IL-2 binding and enabled us to study IL-2 binding in cells that significantly expressed the transgene. We quantified ^{125}I-labeled IL-2 binding on IL-2Rβ-transfected COS-7 cells showing that the IL-2 *Kd* is about the same as for the well known, intermediate affinity receptor, IL-2Rβ/γc heterodimer, and for the IL-2Rβ/β homodimer.

IL-2Rβ homodimers may represent either a decoy receptor or a new form of the IL-2R able to induce signals. Previously published data and preliminary results favour the second hypothesis. We have shown that peptide P1-30, which selectively binds to IL-2Rβ, activates NK cells which overexpress this chain [25, 26]. By comparison with IL-2R signalling [36-39], others have studied the properties of chimeras, where IL-2Rβ cytoplasmic domains were fused to extracellular domains from homodimeric systems such as c-Kit:IL-2Rβ, prolactinR:IL-2Rβ and EPOR:IL-2Rβ [40, 41]. In the presence of the corresponding growth factor, IL-2Rβ cytoplasmic domain pairs were brought together and induced protein phosphorylation. Thus, as a preliminary approach, we conducted a study using monocytes from an infant with SCID caused by a missense mutation truncating the γc chain (R289stop). This stop-mutation, six residues downstream of the putative transmembrane alpha-helix (residues 263-283), causes the entire cytoplasmic domain (residues 289-369) to be missing. Monocytes from this patient, stimulated by IL-2, produced large amounts of IL-8 (unpublished data). The shortened γc mutant was expressed at the cell surface and might interact with IL-2Rβ. However, in the absence of the cytoplasmic domain, the shortened γc cannot contribute to signaling. One of the possible explanations is that the IL-2-response observed might be mediated by IL-2Rβ homodimers.

Our finding may have some relevance in the activation of NK cells, which are an important part of immune system defenses against virus-infected cells and tumor cells. Quiescent NK cells ($CD56^+$ $CD16^+$ $CD69^-$ $CD25^-$) constitutively express IL-2Rβ at their surface, whereas only weak production of γc chain is observed [42, 43]. The ratio of their surface expressions was measured by FACS, showing that 17-fold more IL-2Rβ is expressed than γc. The ratio of their mRNA expressions was evaluated by quantitative PCR, showing that 12-fold more IL-2Rβ mRNA is produced than γc. The precise mechanisms controlling the constitutive responsiveness of NK lymphocytes to IL-2 have not been fully elucidated. Here, we report on the biochemical ability of IL-2Rβ chains to form homodimers, and since these chains are present in excess at the surface of NK cells, it may be hypothesized that these dimeric molecules are present on their surface in addition to less common IL-2Rβ/γc heterodimeric complexes. During the early stages of NK cell activation, if these homodimers have functional activities they might contribute to triggering signaling pathways after IL-2 and IL-15 stimulation. This may represent an initiator or an amplifier of the early IL-2 response in NK cells.

The results presented here show that IL-2Rβ subunits form homodimers, with an intermediate affinity for IL-2 as described for the heterodimer IL-2Rβ/γc. The function and mode of action of this homodimer that might be important at the surface of NK lymphocytes need further investigation.

Acknowledgments. *The authors wish to thank Prof. Alain Fischer and Dr. Nizar Mahlaoui (Hôpital Necker, Paris) for providing SCID patient blood samples. We are very grateful to Dr. Sandra Pellegrini and Prof. James Di Santo (Institut Pasteur, Paris) for their advice and useful discussions during the experimental work performed and in the preparation of the manuscript. We also wish to thank Dr. Yannick Jacques (INSERM, Nantes) for providing the anti-IL-2Rβ A41 mAb. We thank Pascal Roux (Plate-Forme d'Imagerie Dynamique, Institut Pasteur) for his expertise and technical help in confocal microscopy.. A.-H.P., O.J. and V.M.-P. contributed equally to this work. A.-H.P. is supported by a fellowship from the Ministère de l'Education Nationale et de la Recherche. O.J. and V.M.-P. are supported by grants from the Agence Nationale de*

Recherches sur le SIDA (ANRS). F.G. joined the INSERM U461, Faculté de Pharmacie, Chatenay-Malabry and P.C. joined the Unité de Biologie Moléculaire de l'Expression Génique, Institut Pasteur Paris.

REFERENCES

1. Taniguchi T, Matsui H, Fujita T, *et al.* Structure and expression of cloned cDNA for human interleukin-2. *Nature* 1983; 302: 305.
2. Smith KA. Interleukin-2: inception, impact, and implications. *Science* 1988; 240: 1169.
3. Theze J, Alzari PM, Bertoglio J. Interleukin 2 and its receptors: recent advances and new immunological functions. *Immunol Today* 1996; 17: 481.
4. Leonard WJ. In: Oppenheim J, Feldman M, eds. *Cytokine Reference*. Academic Press, 2001: 1339.
5. Schorle H, Holtschke T, Hunig T, *et al.* Development and function of T cells in mice rendered interleukin-2 deficient by gene targeting. *Nature* 1991; 352: 621.
6. Chastagner P, Reddy J, Theze J. Lymphoadenopathy in IL-2-deficient mice: further characterization and overexpression of the antiapoptotic molecule cellular FLIP. *J Immunol* 2002; 169: 3644.
7. Lenardo MJ. Interleukin-2 programs mouse alpha beta T lymphocytes for apoptosis. *Nature* 1991; 353: 858.
8. Malek TR, Bayer AL. Tolerance, not immunity, crucially depends on IL-2. *Nat Rev Immunol* 2004; 4: 665.
9. Uchiyama T, Broder S, Waldmann TA. A monoclonal antibody (anti-Tac) reactive with activated and functionally mature human T cells. I. Production of anti-Tac monoclonal antibody and distribution of Tac (+) cells. *J Immunol* 1981; 126: 1393.
10. Leonard WJ, Depper JM, Crabtree GR, *et al.* Molecular cloning and expression of cDNAs fort he human interleukin-2 receptor. *Nature* 1984; 311: 626.
11. Teshigawara K, Wang HM, Kato K, *et al.* Interleukin 2 high-affinity receptor expression requires two distinct binding proteins. *J Exp Med* 1987; 165: 223.
12. Hatakeyama M, Tsudo M, Minamoto S, *et al.* Interleukin-2 receptor beta chain gene: generation of three receptor forms by cloned human alpha and beta chain cDNAs. *Science* 1989; 244: 551.
13. Tsudo M, Kitamura F, Miyasaka M. Characterization of the interleukin 2 receptor beta chain using three distinct monoclonal antibodies. *Proc Natl Acad Sci USA* 1989; 86: 1982.
14. Takeshita T, Asao H, Ohtani K, *et al.* Cloning of the gamma chain of the human IL-2 receptor. *Science* 1992; 257: 379.
15. Adriani M, Garbi C, Amodio G, *et al.* Functional interaction of common gamma-chain and growth hormone receptor signaling apparatus. *J Immunol* 2006; 177: 6889.
16. Giri JG, Kumaki S, Ahdieh M, *et al.* Identification and cloning of novel IL-15 binding protein that is structurally related to the alpha chain of the IL-2 receptor. *EMBO J* 1995; 14: 3654.
17. Gesbert F, Delespine-Carmagnat M, Bertoglio J. Recent advances in the understanding of the interleukin-2 signal transduction. *J Clin Immunol* 1998; 18: 307.
18. Ellery JM, Nicholls PJ. Alternate signaling pathway from the interleukin-2 receptor. *Cytokine Growth Factor Rev* 2002; 13: 27.
19. Yamaoka K, Saharinen P, Pesu M, Silvennoinen 3rd O, O'Shea JJ. The Janus kinases (Jaks). *Genome Biol* 2004; 5: 253.
20. Leonard WJ, O'Shea JJ. Jaks and STATs: biological implications. *Annu Rev Immunol* 1998; 16: 293.
21. Lin JX, Leonard WJ. The role of Stat5a and Stat5b in signaling by IL-2 family cytokines. *Oncogene* 2000; 19: 2566.
22. Wang X, Rickert M, Garcia KC. Structure of the quaternary complex of interleukin-2 with its alpha, beta, and gamma c receptors. *Science* 2005; 310: 1159.
23. Stauber DJ, Debler E, Horton P, *et al.* Crystal structure of the IL-2 signaling complex: paradigm for a heterotrimeric cytokine receptor. *Proc Natl Acad Sci USA* 2006; 103: 2788.
24. Rickert M, Boulanger MJ, Gotiatcheva N, *et al.* Compensatory energetic mechanisms mediating the assembly of signaling complexes between interleukin-2 and its alpha, beta, gamma(c) receptors. *J Mol Biol* 2004; 339: 1115.
25. Eckenberg R, Rose T, Moreau JL, *et al.* The first alpha helix of interleukin (IL)-2 folds as a homotetramer, acts as an agonist of the IL-2 receptor beta chain, and induces lymphokine-activated killer cells. *J Exp Med* 2000; 191: 529.
26. Rose T, Moreau JL, Eckenberg R. Structural analysis and modeling of a synthetic interleukin-2 mimetic and its interleukin-2Rbeta2 receptor. *J Biol Chem* 2003; 278: 22868.
27. Hori T, Uchiyama T, Tsudo M, *et al.* Establishment of an interleukin 2-dependent human T cell line from a patient with T cell chronic lymphocytic leukemia who is not infected with human T cell leukemia/lymphoma virus. *Blood* 1987; 70: 1069.
28. Wouter FS, Bastiaens PI. Imaging protein-protein interactions by fluorescence resonance energy transfer microscopy. In: Coligan JE, Dunn BM, Speicher DW, Wingfield PT, eds. *Current Protocols in Protein Science*. John Wiley & Sons, 2001; (19.5.1-15).
29. Bastiaens PI, Majoul IV, Verveer PJ, *et al.* Imaging the intracellular trafficking and state of the AB5 quaternary structure of cholera toxin. *EMBO J* 1996; 15: 4246.
30. He L, Bradrick TD, Karpova TS, *et al.* Flow cytometric measurement of florescence (Forster) resonance energy transfer from cyan fluorescent protein to yellow fluorescent protein using single-laser excitation at 458 nm. *Cytometry A* 2003; 53: 39.
31. Schumacher TNM, Tsomides TJ. *In Vitro* Radiolabeling of Peptides and Proteins. In: Coligan JE, Dunn BM, Speicher DW, Wingfield PT, eds. *Current Protocols in Protein Science*. John Wiley & Sons, 2003; (3.3.1).
32. David D, Bani L, Moreau JL, *et al.* Further analysis of interleukin-2 receptor subunit expression on the different human peripheral blood mononuclear cell subsets. *Blood* 1998; 91: 165.
33. Damjanovich S, Bene L, Matko J, *et al.* Preassembly of interleukin 2 (IL-2) receptor subunits on resting Kit 225 K6 T cells and their modulation by IL-2, IL-7, and IL-15: a fluorescence resonance energy transfer study. *Proc Natl Acad Sci USA* 1997; 94: 13134.
34. Takeshita T, Ohtani K, Asao H, *et al.* An associated molecule, p64, with IL-2 receptor beta chain. Its possible involvement in the formation of the functional intermediate-affinity IL-2 receptor complex. *J Immunol* 1992; 148: 2154.
35. Liparoto SF, Myszka DG, Wu Z, *et al.* Analysis of the role of the interleukin-2 receptor gamma chain in ligand binding. *Biochemistry* 2002; 41: 2543.
36. Tanaka N, Asao H, Ohbo K, *et al.* Physical association of JAK1 and JAK2 tyrosine kinases with the interleukin 2 receptor beta and gamma chains. *Proc Natl Acad Sci USA* 1994; 91: 7271.
37. Kirken RA, Rui H, Malabarba MG, *et al.* Activation of JAK3, but not JAK1, is critical for IL-2-induced proliferation and STAT5 recuitment by a COOH-terminal region of the IL-2 receptor beta-chain. *Cytokine* 1995; 7: 689.

38. Stahl N, Yancopoulos GD. The alphas, betas, and kinases of cytokine receptor complexes. *Cell* 1993; 74: 587.

39. Nelson BH, Lord JD, Greenberg PD. Cytoplasmic domains of the interleukin-2 receptor beta and gamma chains mediate the signal for T cell proliferation. *Nature* 1994; 369: 333.

40. Jiang N, He TC, Miyajima A, *et al.* The box1 domain of the erythropoietin receptor specifies Janus kinase 2 activation and functions mitogenically within an interleukin 2 beta-receptor chimera. *J Biol Chem* 1996; 271: 16472.

41. Ferrag F, Pezet A, Chiarenza A, *et al.* Homodimerization of IL-2 receptor beta chain is necessary and sufficient to activate Jak2 and downstream signaling pathways. *FEBS Lett* 1998; 421: 32.

42. Siegel JP, Sharon M, Smith PL, *et al.* The IL-2 receptor beta chain (p70): role in mediating signals for LAK, NK, and proliferative activities. *Science* 1987; 238: 75.

43. David D, Bani L, Moreau C, *et al.* Further analysis of interleukin-2 receptor subunit expression on the different human peripheral blood mononuclear cells subsets. *Blood* 1998; 91: 165-72.